

4×4 multiple-input multiple-output coherent microwave photonic link with optical independent sideband and optical orthogonal modulation

(Invited Paper)

Xiang Chen and Jianping Yao*

Microwave Photonics Research Laboratory, School of Electrical Engineering and Computer Science,
University of Ottawa, Ottawa, Ontario K1N 6N5, Canada

*Corresponding author: jpyao@uottawa.ca

Received October 14, 2016; accepted December 15, 2016; posted online January 9, 2017

A 4×4 multiple-input multiple-output coherent microwave photonic (MWP) link to transmit four wireless signals with an identical microwave center frequency over a single optical wavelength based on optical independent sideband (OISB) modulation and optical orthogonal modulation with an improved spectral efficiency is proposed and experimentally demonstrated. At the transmitter, the OISB modulation and optical orthogonal modulation are implemented to generate an OISB signal using a dual-parallel Mach-Zehnder modulator (DP-MZM) driven by four microwave orthogonal frequency-division multiplexing (OFDM) signals with an identical microwave center frequency. At the receiver, the OISB signal is coherently detected at a coherent receiver where a free-running local oscillator (LO) laser source is employed. Digital signal processing is then used to recover the four OFDM signals, to eliminate the phase noise from the transmitter laser source and the LO laser source, and to cancel the unstable wavelength difference between the wavelengths of the transmitter laser source and the LO laser source. Error-free transmission of three 16 quadrature amplitude modulation (16-QAM) 1 Gbps OFDM signals and one 16-QAM 1.5 Gbps OFDM signal at a microwave center frequency of 2.91 GHz over a 10 km single-mode fiber is experimentally demonstrated.

OCIS codes: 060.0060, 060.5625, 060.2840.

doi: 10.3788/COL201715.010008.

The transmission of microwave signals over an optical fiber, or a microwave photonic (MWP) link, has been considered as a simple, low cost, and low-power-consumption solution for broadband wireless signal transmission^[1,2]. Such links also enable a centralized radio access network (C-RAN) architecture, which can reduce the network complexity and system cost, offering improved network performance via coordinated multipoints and improved network energy efficiency^[3]. In addition, in a C-RAN the central stations (CSs) are located in physically secured locations, thus internet protocol security for the links between the CSs and the core network is no longer needed. On the other hand, to meet the requirement of a huge amount of mobile and wireless local area network data and enable multiple-input multiple-output (MIMO)—a key technology for the fifth-generation (5G), MWP links are required to transmit multiple wireless signals over a single fiber. One solution is to transmit digitized in-phase (I) and quadrature (Q) components of multiple wireless signals in a binary sequence via time-division multiplexing (TDM), which is widely used in today's mobile fronthaul^[3-5]. Although such a technique can offer excellent robustness against noise, the spectral efficiency is very low since ON-OFF-keying (OOK) modulation format is employed^[6]. In addition, the use of TDM inherently limits the performance in terms of the latency of the system. To improve the bandwidth efficiency and decrease the latency, the transmission of multiple wireless

signals via frequency-division multiplexing (FDM) in a single wavelength has been proposed^[6-8]. The main disadvantage of the two solutions^[3-5] is that at the remote radio head (RRH) electrical local oscillators (ELOs) with different frequencies for different wireless signals used to realize frequency conversion are required, making the RRH very costly. To avoid using ELOs at the RRH several schemes have been proposed^[9,10]. In Ref. [9], a simple 2×2 MIMO orthogonal frequency division multiplex (OFDM) MWP link employing single-sideband modulation was proposed that can tolerate the chromatic dispersion existing in the fiber link. To cancel the high peak-to-average-power ratio due to the OFDM modulation^[9], single-sideband single-carrier modulation, which has a lower peak-to-average-power ratio, was employed^[10]. For both schemes, to realize a 2×2 MIMO MWP link, multiple optical wavelengths to carry different wireless signals have to be employed^[9,10]. Thus, multiple optical wavelengths, multiple modulators, and multiple photodiodes (PDs) have to be used, which would make the system complicated and costly. In addition, the spectral efficiency for each channel (each wavelength) is very low. To simplify the system, increase the spectral efficiency, and avoid using ELOs at the RRH, several MIMO optical-wireless integration systems have been proposed in which optical polarization multiplexing has to be employed. For example, a 2×2 MIMO MWP link implemented using two orthogonally polarized optical light

waves to carry two microwave signals was reported^[11–13]. Recently, we proposed two schemes to transmit two independent microwave vector signals with an identical microwave center frequency in a single wavelength based on coherent detection for a 2×2 MIMO MWP link^[14,15]. However, there are several disadvantages for the two schemes in Refs. [14,15]. First, in Ref. [14], the phase noise introduced by the transmitter laser source was not cancelled, which may degrade the transmission performance. Second, in Refs. [14,15], an unmodulated optical carrier that has a polarization state orthogonal to the modulated optical signal is transmitted to the receiver side for coherent detection. Since the two orthogonal polarization states are used, polarization multiplexing cannot be implemented, which would reduce the transmission capacity and decrease the optical energy efficiency. In addition, in Ref. [14], since the unmodulated optical carrier from the transmitter is used as an optical local oscillator (LO) for coherent detection, it has to be amplified at the receiver by an optical amplifier to satisfy the power level needed for coherent detection, which may add an additional noise to the link.

In this Letter, an MWP link to transmit four wireless signals with an identical microwave center frequency without using FDM over a single optical wavelength based on optical independent sideband (OISB) modulation and optical orthogonal modulation incorporating optical coherent detection and digital signal processing (DSP) is proposed and experimentally demonstrated. In the proposed scheme, four independent microwave signals are transmitted to the receiver, which enables 4×4 MIMO and no ELOs are needed at the RRH for frequency conversion. Compared with the schemes in Refs. [3–8], due to the use of OISB modulation, optical orthogonal modulation and coherent detection that can detect both the phase and intensity information of optical signals are employed, the spectral efficiency and the number of transmitted wireless signals for each channel (or wavelength) is increased. In addition, the LO is not from the transmitter, no optical amplifier is needed, and no additional noise from the optical amplifier will be introduced. Furthermore, since the remote LO is replaced by an LO at the receiver side, polarization multiplexing can be employed that would enable 8×8 MIMO. In addition, since the four microwave signals are with an identical microwave center frequency, more microwave signals using FDM could be transmitted, thus the data rate could be further increased. Finally, the phase noise and unstable frequency difference introduced by the transmitter laser source and the LO laser source are cancelled by a DSP-based phase noise cancellation unit. A proof-of-concept experiment is performed. Three 1 Gbps OFDM signals and a 1.5 Gbps OFDM signal all with 16 quadrature amplitude modulation (16-QAM) at an identical microwave carrier frequency of 2.91 GHz modulated on a single optical carrier are transmitted over a 10 km single-mode fiber (SMF). When the received optical power is only -20.3 dBm, the raw bit error rates (BERs) of the four wireless signals are still less than 3×10^{-3} , which enables

error-free transmission if the state-of-the-art forward error correction (FEC) technique is employed.

Figure 1 shows the schematic of the proposed coherent MWP link based on OISB modulation and optical orthogonal modulation. A continuous-wave (CW) light from a laser diode (LD) is sent to a dual-parallel Mach–Zehnder modulator (DP-MZM), which consists of three MZMs (two sub-MZMs, sub-MZM1 and sub-MZM2, and one main MZM). The main MZM is biased at the quadrature point and the sub-MZM2 is biased at the null point while sub-MZM1 is low biased. Two microwave signals are applied to the DP-MZM via the two electrodes. At the output of the DP-MZM, two optical pilot tones, an optical carrier and an OISB signal that contains four microwave OFDM signals, are generated. Each sideband carries two OFDM signals whose optical subcarriers are orthogonal. After a 10 km SMF transmission, the OISB signal is coherently detected at the receiver. After DSP, the four microwave OFDM signals are separated and the phase noise and unstable frequency difference between the transmitter laser source and the LO laser source are cancelled. In the signal processing unit, no ELOs are needed.

Figure 2 shows the principle of the dual independent sideband generation with four real OFDM signals. First, four baseband real OFDM signals, which are individually vector mapped, are generated. Note, the modulation format, the symbol rate, the bandwidth, and the number of subcarriers of each real OFDM signal can be different. Second, the four baseband OFDM signals $S_1(t)$, $S_2(t)$, $S_3(t)$, and $S_4(t)$, modulate the RF carriers in a complex sinusoidal form. $S_1(t)$ is carried by the positive frequency carrier in the form of $\exp(j\omega_{RF}t)$, $S_2(t)$ is carried by the carrier

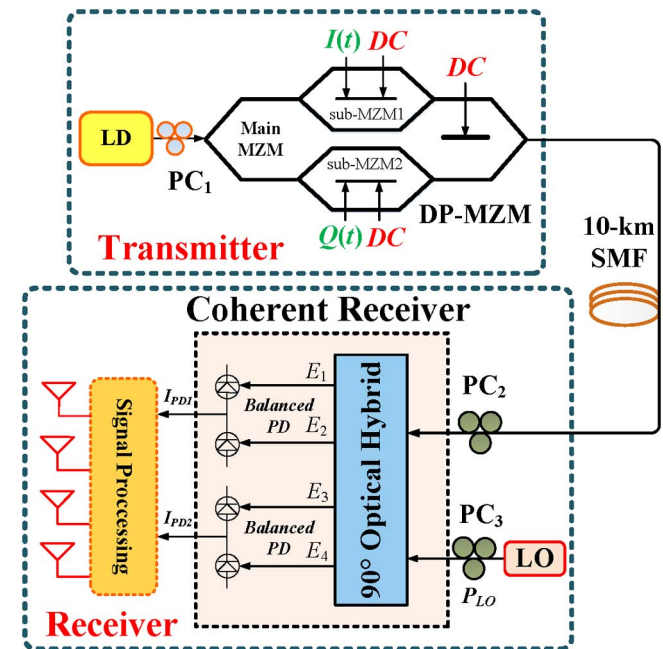


Fig. 1. Schematic diagram of the proposed coherent MWP link based on OISB modulation and optical orthogonal modulation. PC: polarization controller.

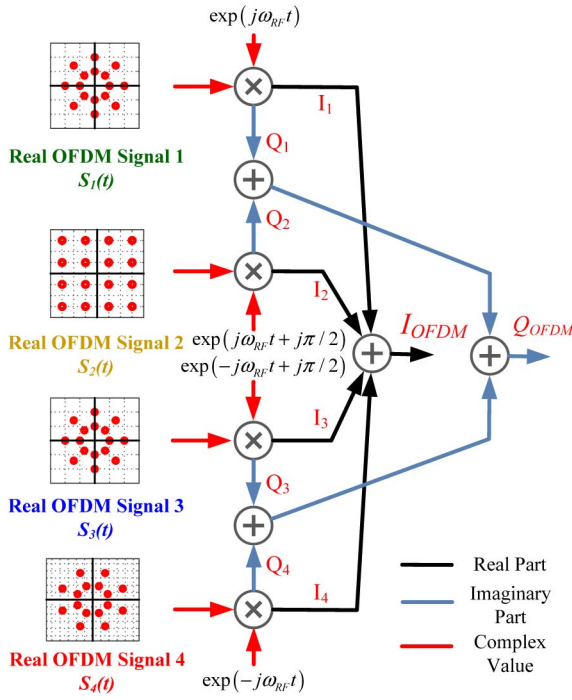


Fig. 2. Principle of dual independent sideband generation with four real OFDM signals.

with the same frequency having a $\pi/2$ initial phase, which is expressed as $\exp(j\omega_{RF}t + \pi/2)$. Apparently, the RF carriers of the two signals are orthogonal. For $S_3(t)$ and $S_4(t)$, the two baseband signals are upconverted to the same intermediate frequency on the negative side. The two carriers for $S_3(t)$ and $S_4(t)$ can be expressed as $\exp(-j\omega_{RF}t)$ and $\exp(-j\omega_{RF}t + \pi/2)$. Again, they are also orthogonal. Note that in the proposed scheme the frequencies of the four carriers can be equal or not equal. Then, the real parts and imaginary parts of the four complex microwave OFDM signals are added together. Figure 3 shows the spectrum of the complex signal after the four complex microwave OFDM signals are combined. As can be seen, the upper sideband contains OFDM signal 1 and OFDM signal 2 and the lower sideband contains OFDM signal 3 and OFDM signal 4. Figure 4 shows the insertion of a pilot tone with an angular frequency of $2\omega_{RF}$, which is combined with the real parts of the complex microwave OFDM signals and used to separate the four OFDM signals at the receiver side. Figure 5 shows the spectrum of the OFDM signals with the added pilot tone. Since the

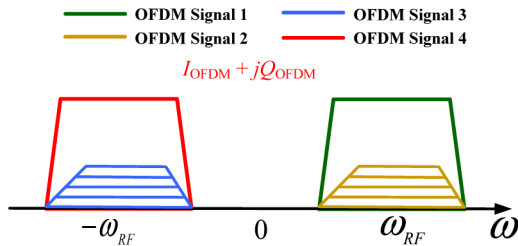


Fig. 3. Spectrum of the two independent sideband signals with four real OFDM signals.

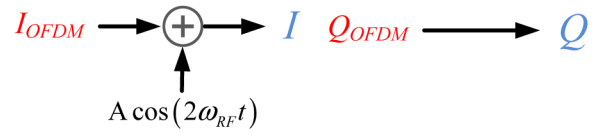


Fig. 4. Schematic diagram to show the pilot-tone insertion.

pilot tone is a real signal, the spectrum of the pilot tone is Hamilton symmetric. Finally, the real part and imaginary part of the combined complex signal, shown in Fig. 5, are applied to the DP-MZM via the two electrodes. To generate an OISB signal, the bias points of the three MZMs inside the DP-MZM are biased as follows: the main MZM is biased at the quadrature point, sub-MZM2 is biased at the null point, and sub-MZM1 is low biased. Mathematically, the optical field at the output of the DP-MZM is given by

$$E_s(t) = \frac{\sqrt{2P_s L_s}}{2} \left[\cos(\pi I(t)/2V_{\pi RF} + \alpha) e^{j(\omega_c t + \varphi_c(t))} + \sin(\pi Q(t)/2V_{\pi RF}) e^{j(\omega_c t + \varphi_c(t) + \varphi_{DC})} \right] \approx \frac{\sqrt{2P_s L_s}}{2} \left\{ \begin{array}{l} \left[\cos(\alpha) \right. \\ \left. -\pi \sin(\alpha) I(t)/2V_{\pi RF} \right] e^{j(\omega_c t + \varphi_c(t))} \\ \left. + \pi Q(t)/2V_{\pi RF} \cdot e^{j(\omega_c t + \varphi_c(t) + \varphi_{DC})} \right\}, \quad (1)$$

where P_s is the optical power at the input of the DP-MZM, ω_c is the angular frequency of the light wave, $\varphi_c(t)$ is the phase term of the transmitter laser source, $V_{\pi DC}$ is the half-wave voltage of the DP-MZM at DC, φ_{DC} is the phase difference between the two arms of the main MZM, L_s is the link loss between the coherent receiver and the transmitter, $I(t)$ is the real part of the complex signal, and $Q(t)$ is the imaginary part of the complex signal. The phase difference $\alpha = \pi V_{bias}/2V_{\pi DC}$ between the two arms of sub-MZM1 is controlled by a DC bias V_{bias} . Both $I(t)$ and $Q(t)$ are small signals and can be expressed as

$$I(t) = S_1(t) \cdot \cos(\omega_{RF}t) - S_2(t) \cdot \sin(\omega_{RF}t) + S_3(t) \cdot \sin(\omega_{RF}t) + S_4(t) \cdot \cos(\omega_{RF}t) + A \cos(2\omega_{RF}t), \quad (2)$$

$$Q(t) = I \left[\begin{array}{l} S_1(t) \cdot \sin(\omega_{RF}t) + S_2(t) \cdot \cos(\omega_{RF}t) \\ + S_3(t) \cdot \cos(\omega_{RF}t) - S_4(t) \cdot \sin(\omega_{RF}t) \end{array} \right], \quad (3)$$

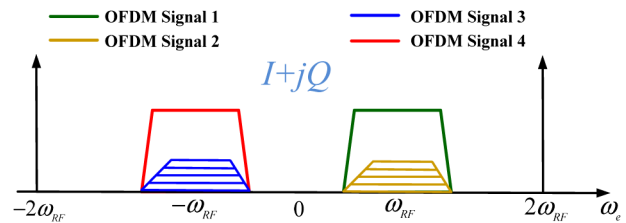


Fig. 5. Spectrum of the two independent sideband signals with the pilot tone.

where $S_1(t)$, $S_2(t)$, $S_3(t)$, and $S_4(t)$ are the four baseband real OFDM signals, ω_{RF} is the center frequency of the four microwave OFDM signals, A is the amplitude of the electrical pilot tone, and l is an attenuation factor. To generate an OISB signal, the optical power for the two optical sidebands at the output of sub-MZM1 ($[\pi \sin(\alpha)I(t)/2V_{\pi\text{RF}}] \exp[j(\omega_c t + \varphi_c(t))]$) and sub-MZM2 ($[\pi Q(t)/2V_{\pi\text{RF}}] \exp[j(\omega_c t + \varphi_c(t) + \varphi_{\text{DC}})]$) should be equal, thus l should be equal to $\sin(\alpha)$, which is done in the system by decreasing the electrical power of $Q(t)$. Since the main MZM is biased at the quadrature point, φ_{DC} can be equal to either $\pi/2$ or $-\pi/2$. Figure 6 shows the optical spectrum of the OISB signal at the output of the DP-MZM when φ_{DC} is equal to $-\pi/2$. It can be seen that the signals shown in Fig. 5 are frequency upconverted to ω_c . In addition, optical orthogonal modulation is realized. Each sideband contains two OFDM signals whose optical subcarriers are orthogonal. Figure 7 shows the optical spectrum of the OISB signal at the output of the DP-MZM when φ_{DC} is equal to $\pi/2$. The only difference between the signals shown in Figs. 6 and 7 is that the positions of the signals at the lower and the upper sidebands are swapped. In addition, to separate the four microwave OFDM signals at the receiver side, the optical carrier is partially suppressed to make it have a power identical to that of either of the two pilot tones. In the following analysis, we assume that φ_{DC} is equal to $\pi/2$.

After transmission over an SMF, the optical signal is coherently detected by a coherent receiver while a free-running LO laser source is used as an LO source. The optical field of the light wave from the LO laser source is given by

$$E_{\text{LO}}(t) = \sqrt{2P_{\text{LO}}} e^{j(\omega_{\text{LO}}t + \varphi_{\text{LO}}(t))}, \quad (4)$$

where P_{LO} is the optical power, $\varphi_{\text{LO}}(t)$ is the phase term, and ω_{LO} is the angular frequency.

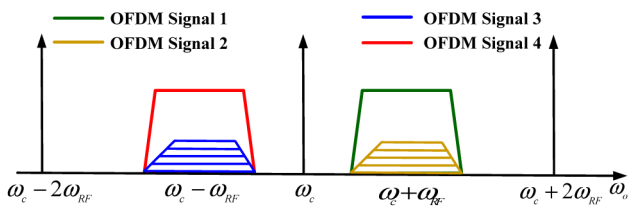


Fig. 6. Optical spectrum at the output of the DP-MZM for $\varphi_{\text{DC}} = -\pi/2$.

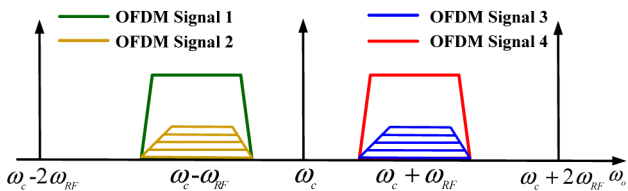


Fig. 7. Optical spectrum at the output of the DP-MZM for $\varphi_{\text{DC}} = \pi/2$.

The optical signal from the transmitter and the light wave from the LO laser source are co-polarized and are applied to a 90° optical hybrid. At the four outputs of the 90° optical hybrid, we have four optical signals with the electrical fields given by

$$E_1 = \sqrt{L}(E_s + E_{\text{LO}}), \quad (5)$$

$$E_2 = \sqrt{L}(E_s - E_{\text{LO}}), \quad (6)$$

$$E_3 = \sqrt{L}(E_s + E_{\text{LO}} e^{j\pi/2}), \quad (7)$$

$$E_4 = \sqrt{L}(E_s - E_{\text{LO}} e^{j\pi/2}), \quad (8)$$

where L is the insertion loss caused by the 90° optical hybrid.

By applying E_1 and E_2 , and E_3 and E_4 , to two balanced photodetectors we have two output photocurrents given by

$$I_{\text{PD1}} = 2RL\sqrt{P_s P_{\text{LO}}} L_s (I_{\text{EC1}} + I_{\text{PR1}} + I_{\text{PL1}} + S_{\text{lower1}} + S_{\text{upper1}}), \quad (9)$$

$$I_{\text{EC1}} = \cos(\alpha) \cos[(\Delta\omega)t + \varphi(t)],$$

$$I_{\text{PR1}} = -0.5AB \cos[(\Delta\omega)t + \varphi(t) + 2\omega_{\text{RF}}t],$$

$$I_{\text{PL1}} = -0.5AB \cos[(\Delta\omega)t + \varphi(t) - 2\omega_{\text{RF}}t],$$

$$S_{\text{lower1}} = -BS_1(t) \cos[(\Delta\omega)t + \varphi(t) - \omega_{\text{RF}}t] - BS_2(t) \cdot \sin[(\Delta\omega)t + \varphi(t) - \omega_{\text{RF}}t],$$

$$S_{\text{upper1}} = -BS_3(t) \sin[(\Delta\omega)t + \varphi(t) + \omega_{\text{RF}}t] - BS_4(t) \cos[(\Delta\omega)t + \varphi(t) + \omega_{\text{RF}}t],$$

$$B = \pi l/2V_{\pi\text{RF}} = \pi \sin(\alpha)/2V_{\pi\text{RF}},$$

and

$$I_{\text{PD2}} = 2RL\sqrt{P_s P_{\text{LO}}} L_s (I_{\text{EC2}} + I_{\text{PR2}} + I_{\text{PL2}} + S_{\text{lower2}} + S_{\text{upper2}}), \quad (10)$$

$$I_{\text{EC2}} = \cos(\alpha) \sin[(\Delta\omega)t + \varphi(t)],$$

$$I_{\text{PR2}} = -0.5AB \sin[(\Delta\omega)t + \varphi(t) + 2\omega_{\text{RF}}t],$$

$$I_{\text{PL2}} = -0.5AB \sin[(\Delta\omega)t + \varphi(t) - 2\omega_{\text{RF}}t],$$

$$S_{\text{lower2}} = -BS_1(t) \sin[(\Delta\omega)t + \varphi(t) - \omega_{\text{RF}}t] + BS_2(t) \cos[(\Delta\omega)t + \varphi(t) - \omega_{\text{RF}}t],$$

$$S_{\text{upper2}} = BS_3(t) \cos[(\Delta\omega)t + \varphi(t) + \omega_{\text{RF}}t] - BS_4(t) \sin[(\Delta\omega)t + \varphi(t) + \omega_{\text{RF}}t],$$

$$B = \pi l/2V_{\pi\text{RF}} = \pi \sin(\alpha)/2V_{\pi\text{RF}},$$

where $\Delta\omega = \omega_c - \omega_{\text{LO}}$ is the frequency difference between the transmitter and the LO laser sources, $\varphi(t)$ is the phase noise introduced by the transmitter laser source and the LO laser source, $\varphi(t) = \varphi_c(t) - \varphi_{\text{LO}}(t)$, and R is the responsivity of the PD. As can be seen, the photocurrent I_{PD1} contains one electrical carrier (I_{EC1}), one left pilot tone (I_{PL1}),

one right pilot tone (I_{PR1}), and four microwave OFDM signals. Apparently, the lower sideband (S_{lower1}) contains two OFDM signals that are orthogonal. The same for the two signals in the upper sideband (S_{upper1}). For I_{PD2} , it also contains one electrical carrier (I_{EC2}), one left pilot tone (I_{PL2}), one right pilot tone (I_{PR2}), the lower sideband (S_{lower2}) including $S_1(t)$ and $S_2(t)$, and the upper sideband (S_{upper2}), which contains $S_3(t)$ and $S_4(t)$.

Then, the two photocurrents (I_{PD1} and I_{PD2}) are sent to the DSP unit where the four microwave OFDM signals are separated and the phase noise from the transmitter and the LO laser sources and unstable frequency difference between the transmitter and the LO laser sources are cancelled. Figures 8–11 show the DSP flow charts. First, the electrical

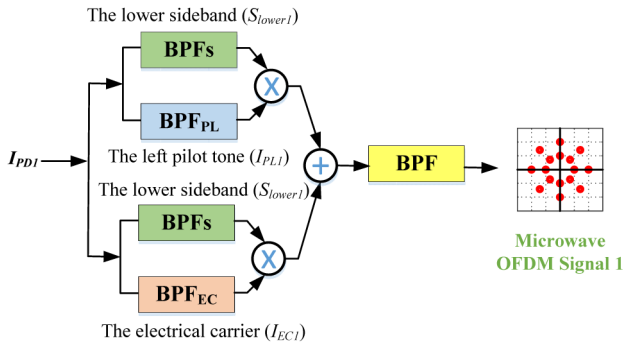


Fig. 8. DSP for recovering microwave OFDM signal 1 and cancelling the phase noise and the unstable frequency difference.

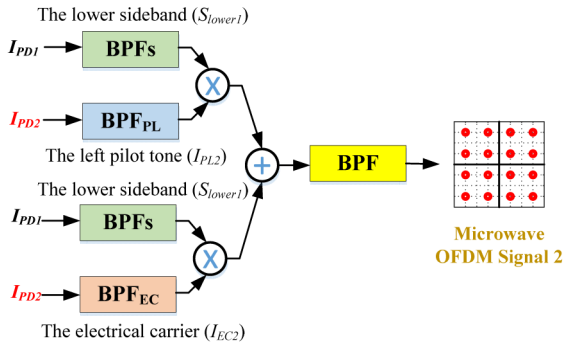


Fig. 9. DSP for recovering microwave OFDM signal 2 and cancelling the phase noise and the unstable frequency difference.

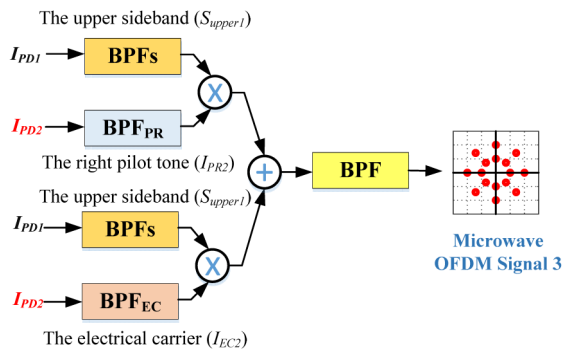


Fig. 10. DSP for recovering microwave OFDM signal 3 and cancelling the phase noise and the unstable frequency difference.

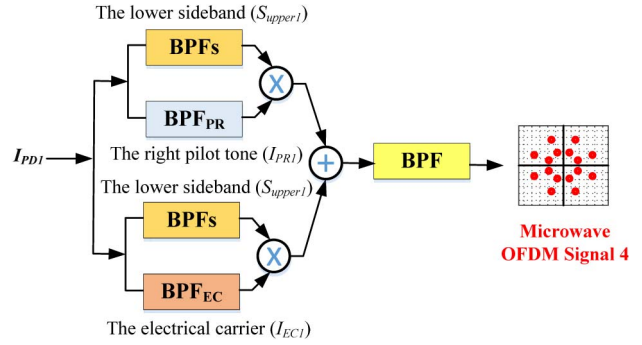


Fig. 11. DSP for recovering microwave OFDM signal 4 and cancelling the phase noise and the unstable frequency difference.

carrier (I_{EC1}), the left pilot tone (I_{PL1}), the right pilot tone (I_{PR1}), the lower sideband (S_{lower1}), and the upper sideband (S_{upper1}) are separated via electrical filters. Through signal processing, we can easily separate the four microwave signals and cancel the phase noise and unstable frequency difference. The detailed signal processing can be expressed by the following expressions.

$$\begin{aligned}
 S_1(t) \cos(\omega_{RF} t) &\propto F[S_{lower1} \cdot I_{EC1} + S_{lower1} \cdot I_{PL1}] \\
 &= -\frac{1}{2} B \left[\cos(\alpha) - \frac{1}{2} AB \right] S_1(t) \cos(\omega_{RF} t) \\
 &\quad - \frac{1}{2} B \left[\cos(\alpha) + \frac{1}{2} AB \right] S_2(t) \sin(\omega_{RF} t),
 \end{aligned} \tag{11}$$

$$\begin{aligned}
 S_2(t) \cos(\omega_{RF} t) &\propto F[S_{lower1} \cdot I_{EC2} + S_{lower1} \cdot I_{PL2}] \\
 &= -\frac{1}{2} B \left(\cos \alpha - \frac{1}{2} AB \right) S_2(t) \cos(\omega_{RF} t) \\
 &\quad - \frac{1}{2} B \left(\cos \alpha + \frac{1}{2} AB \right) S_1(t) \sin(\omega_{RF} t),
 \end{aligned} \tag{12}$$

$$\begin{aligned}
 S_3(t) \cos(\omega_{RF} t) &\propto F[S_{upper1} \cdot I_{EC2} + S_{upper1} \cdot I_{PR2}] \\
 &= -\frac{1}{2} B \left[\cos \alpha - \frac{1}{2} AB \right] S_3(t) \cos(\omega_{RF} t) \\
 &\quad - \frac{1}{2} B \left[-\cos \alpha - \frac{1}{2} AB \right] S_4(t) \sin(\omega_{RF} t),
 \end{aligned} \tag{13}$$

$$\begin{aligned}
 S_4(t) \cos(\omega_{RF} t) &\propto F[S_{upper1} \cdot I_{EC1} + S_{upper1} \cdot I_{PR1}] \\
 &= -\frac{1}{2} B \left[\cos \alpha - \frac{1}{2} AB \right] S_4(t) \cos(\omega_{RF} t) \\
 &\quad - \frac{1}{2} B \left[-\cos \alpha - \frac{1}{2} AB \right] S_3(t) \sin(\omega_{RF} t),
 \end{aligned} \tag{14}$$

where $F[\cdot]$ represents the function of a bandpass filter, which is used to select the microwave OFDM signal. As can be seen in Eqs. (11)–(14), to separate the four microwave

OFDM signals, $\cos(\alpha)$ should be equal to $-0.5BA$. Thus, the power for the electrical carrier and either of the pilot tones is controlled equally. Note that the upper sideband, lower sideband, the carriers, and the pilot tones have the same phase noise and unstable frequency difference introduced from the transmitter and the LO laser sources; through microwave mixing between a sideband and one of the pilot tones or carriers, the phase noise and the unstable frequency difference can be cancelled. As can be seen from Eqs. (11)–(14), the four microwave OFDM signals are free from the phase noise and unstable frequency difference.

To verify that the proposed coherent MWP link can transmit, detect, and separate the four microwave OFDM signals, an experiment is performed based on the setup shown in Fig. 1. A linearly-polarized CW light at 1550.435 nm from a tunable laser source (TLS, Agilent N7714A) with a linewidth of 100 kHz and an optical power of 16 dBm is sent to the DP-MZM (JDSU) via a polarization controller (PC_1). The two signals $I(t)$ and $Q(t)$ applied to the DP-MZM are generated by an arbitrary waveform generator (AWG, Keysight M8915A) with a program composed according to the flow chart shown in Fig. 2 and loaded to the AWG to generate the two signals. Both $I(t)$ and $Q(t)$ contain four different microwave OFDM signals with an identical center frequency at 2.91 GHz. The modulation format for three of the four OFDM signals (OFDM Signal 1, OFDM Signal 3, and OFDM Signal 4) is star 16-QAM. The data rate is 1 Gbps each. The other OFDM signal (OFDM Signal 2) is a rectangular 16-QAM with a data rate of 1.5 Gbps. In the signal $I(t)$ the frequency of the electrical pilot tone is 5.82 GHz and the amplitude is 0.3548 V. As indicated, since $\cos(\alpha)$ should be equal to $-0.5AB$, thus α should be equal to -1.527 . Sub-MZM1 is low biased to introduce a phase shift of -1.527 and sub-MZM2 is biased at the null point, while the main MZM is biased at the quadrature point ($\varphi_{DC} = \pi/2$). The DP-MZM has a bandwidth of 10 GHz and a half-wave voltage of around 6.33 V. Then, the generated OISB signal (the lower sideband carries OFDM Signal 1 and OFDM Signal 2, while the upper sideband carries OFDM Signal 3 and OFDM Signal 4) with two optical pilot tones and an optical carrier are sent to the coherent receiver over a 10 km SMF. At the receiver, coherent detection (Discovery Semiconductors DP-QPSK 40/100 Gbps Coherent Receiver Lab Buddy) with a free running LO laser source (TLS, Yokogawa AQ2201) operating at 1550.485 nm is performed to detect the optical signal. The LO laser source has a linewidth of 1 MHz and an optical power of 9 dBm. Through tuning PC_2 and PC_3 , the light wave from the LO laser source is co-polarized with the received optical signal. Note that in a practical system, PC_2 can be replaced by a dynamic PC, to accommodate the random polarization state of the input optical signal^[10]. At the output of the coherent receiver two photocurrents are generated that are sampled by a digital storage oscilloscope (Agilent DSO-X 93204A) with a sampling rate of 80 GSa/s. Then, the signal is processed offline in a computer.

We would like to point out that, according to the analysis [Eqs. (11) and (14)], the signal processing functions can be realized using pure analog signal processing where analog circuits function as splitters, bandpass filters, and mixers, thus, a high speed analog-to-digital converter (ADC) is not needed. In addition, since no ELOs are needed at the receiver the system, complexity and cost would be significantly reduced.

Figure 12 shows the spectrum of the photocurrent of I_{PD1} . As indicated in Fig. 6 or Fig. 7, the lower sideband contains one 1 Gbps microwave OFDM signal and one 1.5 Gbps microwave OFDM signal (Signal 1 and Signal 2), and the upper sideband contains two 1 Gbps microwave OFDM signals (Signal 3 and Signal 4).

To verify the performance of the coherent MWP link, the error vector magnitude (EVMs) and estimated BERs of the four microwave OFDM signals as a function of received optical power are measured back-to-back and with 10 km fiber transmission. Figure 13 shows the EVMs at different received optical power levels for the four OFDM signals and Fig. 14 shows the BERs at different received optical power levels for the four OFDM signals. As can be seen, after 10 km transmission, even the received optical

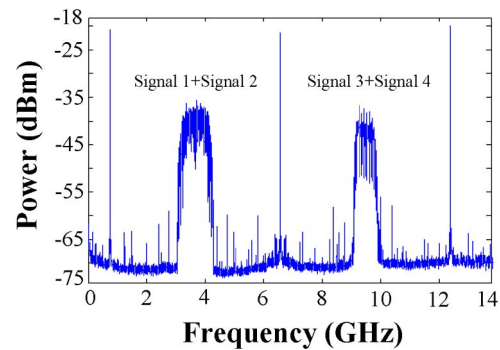


Fig. 12. Spectrum of the signal at the output of the coherent receiver (I_{PD1}).

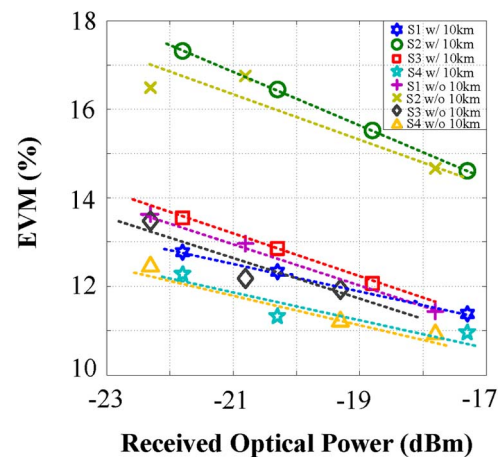


Fig. 13. EVMs at different received optical power levels for the four OFDM signals, S1: Signal 1, S2: Signal 2, S3: Signal 3, S4: Signal 4.

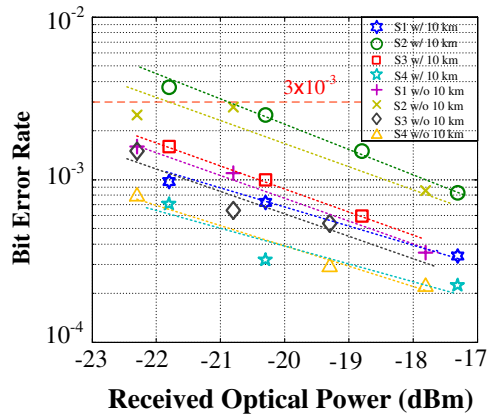


Fig. 14. BERs at different received optical power levels for the four OFDM signals, S1: Signal 1, S2: Signal 2, S3: Signal 3, S4: Signal 4.

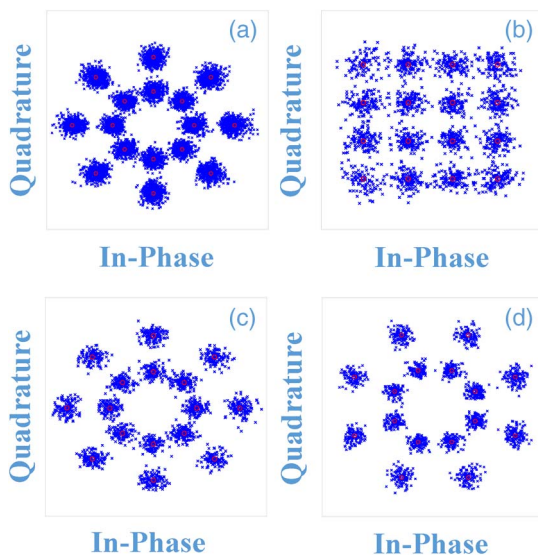


Fig. 15. Measured constellations for the recovered microwave OFDM signals (fiber length: 10 km, the received optical power: -20.3 dBm). (a) Signal 1, (b) Signal 2, (c) Signal 3, and (d) Signal 4.

power is only -20.3 dBm; the raw BERs for the microwave OFDM signals are still less than 3×10^{-3} (FEC threshold, 6.7% overhead), which would enable error-free transmission. The power penalty caused by the fiber transmission is less than 1 dB, which is small and can be ignored. The corresponding constellations of the signals are shown in Fig. 15. As can be seen, the constellations are clear after 10 km transmission, which confirms that the four microwave OFDM signals are well separated and the phase noise and the unstable frequency difference are effectively cancelled. In addition, it can be seen that the power penalty caused by the 10 km SMF transmission is very small, about 1 dB, and can be ignored.

In conclusion, a 4×4 coherent MWP link based on OISB modulation and optical orthogonal modulation is proposed and experimentally demonstrated. The proposed scheme is able to support the transmission of four microwave OFDM signals with an identical center frequency without using electrical FDM and optical wavelength-division multiplexing. If polarization multiplexing is employed, the data transmission capacity would be doubled, that is, eight microwave signals can be transmitted, which would enable 8×8 MIMO. In the proposed scheme, no ELOs are needed for frequency conversion at the receiver, which simplifies significantly the system. In addition, since the OISB modulation and optical orthogonal modulation are employed, the spectral efficiency is improved. The proposed approach is experimentally evaluated. Three 1 Gbps OFDM signals and one 1.5 Gbps OFDM signal at an identical microwave carrier frequency of 2.91 GHz are transmitted over a 10 km SMF. The estimated BERs show that error-free transmission is ensured even for a low received optical power of -20.3 dBm and the power penalty caused by the 10 km fiber is small and can be ignored.

This work was supported by the Natural Sciences and Engineering Research Council of Canada (NSERC).

References

1. J. P. Yao, *J. Lightwave Technol.* **27**, 314 (2009).
2. J. Capmany and D. Novak, *Nat. Photonics* **1**, 319 (2007).
3. A. Pizzinat, P. Chanclou, F. Saliou, and T. Diallo, *J. Lightwave Technol.* **33**, 1077 (2015).
4. J. Wang, Z. Yu, K. Ying, J. Zhang, F. Lu, M. Xu, and G.-K. Chang, in *Proceedings of Optical Fiber Communication Conference* (2016), paper W1H.2.
5. X. Liu, H. Zeng, N. Chand, and F. Effenberger, *J. Lightwave Technol.* **34**, 1556 (2016).
6. X. Liu, F. Effenberger, N. Chand, L. Zhou, and H. Lin, in *Proceedings of Asia Communications Photonics Conference* (2014), paper AF4B.5.
7. X. Liu, F. Effenberger, N. Chand, L. Zhou, and H. Lin, in *Proceedings of Optical Fiber Communication Conference* (2015), paper M2J.2.
8. M. Zhu, X. Liu, N. Chand, F. Effenberger, and G.-K. Chang, in *Proceedings of Optical Fiber Communication Conference* (2015), paper M2J.3.
9. H.-T. Huang, C.-T. Lin, Y.-T. Chiang, C.-C. Wei, and C.-H. Ho, *J. Lightwave Technol.* **32**, 3660 (2014).
10. C.-T. Lin, C.-H. Ho, H.-T. Huang, and Y.-H. Cheng, *Opt. Lett.* **39**, 1358 (2014).
11. J. Yu, X. Li, and N. Chi, *Opt. Express* **21**, 22885 (2013).
12. J. Xiao, J. Yu, X. Li, Y. Xu, Z. Zhang, and L. Chen, *Opt. Lett.* **40**, 998 (2015).
13. N. P. Diamantopoulos, S. Inudo, Y. Yoshida, A. Maruta, A. Kanno, P. T. Dat, T. Kawanishi, R. Maruyama, N. Kuwaki, S. Matsuo, and K. Kitayama, in *Proceedings of Optical Fiber Communication Conference* (2015), paper W4G.2.
14. Y. Chen, T. Shao, A. Wen, and J. P. Yao, *Opt. Lett.* **39**, 1509 (2014).
15. X. Chen and J. P. Yao, *J. Lightwave Technol.* **29**, 3091 (2015).
16. X. S. Yao, L. S. Yan, B. Zhang, A. E. Willner, and J. Jiang, *Opt. Express* **15**, 7407 (2007).